

Scalar Mesons within a model for all non-exotic mesons

Eef van Beveren ^a and George Rupp ^b

^a *Centro de Física Teórica, Departamento de Física,
Universidade, P3004-516 Coimbra, Portugal, (eef@teor.fis.uc.pt)*

^b *Centro de Física das Interações Fundamentais, Instituto Superior Técnico,
Edifício Ciência, P1049-001 Lisboa Codex, Portugal, (george@ajax.ist.utl.pt)*

Contribution to the
Workshop on Recent Developments in Particle and Nuclear Physics
at the
Centro de Física Teórica da Universidade de Coimbra (30/04/2001)

November 28, 2018

Abstract

We describe a four-parameter model for non-exotic meson-meson scattering, which accommodates all non-exotic mesons, hence also the light scalar mesons, as resonances and bound states characterised by complex singularities of the scattering amplitude as a function of the total invariant mass. The majority of the full S -matrix mesonic poles stem from an underlying confinement spectrum. However, the light scalar mesons $K_0^*(830)$, $a_0(980)$, $f_0(400-1200)$, and $f_0(980)$ do not, but instead originate in 3P_0 -barrier semi-bound states.

In the case of bound states, wave functions can be determined. For $c\bar{c}$ and $b\bar{b}$, radiative transitions have been calculated. Here we compare the results to the data.

1 Introduction

Strong interactions have been under study for over half a century by now. Starting from curiosity over nuclear forces [1], they have been developing towards the need to understand Quantum Chromodynamics (QCD) [2]. The modelling and analysis of meson-meson scattering is thereby believed to give valuable contributions. Here we will report on a model for meson-meson scattering which has been very successful in predicting and reproducing a host of experimental data with a very limited number of parameters [3]–[9]. It is based on our perspective of QCD, as outlined below.

Mesons are composed of quarks, antiquarks, and gluons, whether stable with respect to OZI-allowed hadronic decay, i.e., bound states like K , J/ψ , and Υ , or unstable, decaying into two or more lighter mesons, like e.g. the resonances ρ , ω , and ϕ . Mesons can be described by systems of one constituent quark (q) confined to one constituent antiquark (\bar{q}). Constituent quarks and antiquarks, which can be thought of as lumps of bare quarks surrounded by glue and a cloud of virtual $q\bar{q}$ pairs, determine the flavour of the meson and the bulk of its mass. The remaining strong interactions may be parametrised by an effective confining potential, e.g. a harmonic oscillator.

Decay of a meson into a pair of lighter mesons is assumed to be the result of the creation of a new constituent $q\bar{q}$ pair with the quantum numbers of the vacuum (3P_0), leading to OZI-allowed transitions. Mesonic resonances in meson-meson scattering are supposed to be formed through the inverse phenomenon, i.e., the annihilation of a constituent $q\bar{q}$ pair with the quantum numbers of the vacuum, one from each of the two mesons involved in the scattering process.

The spatial quantum numbers (ν, J^{PC}) of a meson, either bound state or resonance, follow from the total spin of the constituent $q\bar{q}$ pair, their relative orbital angular momentum ℓ , and their radial quantum number ν .

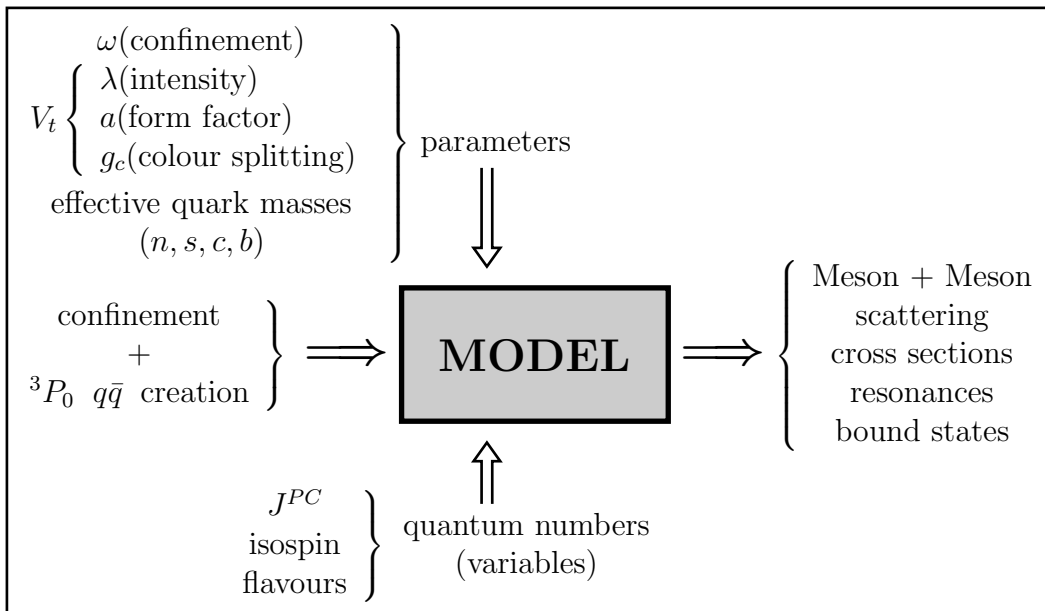


Figure 1: Schematic picture of the model for the description of non-exotic meson-meson scattering.

In Fig. (1) we schematically show how the model for the description of non-exotic meson-

meson scattering works. The employed dynamics is characterised by confinement and 3P_0 $q\bar{q}$ -pair creation. Confinement is provided by a harmonic oscillator potential with universal frequency ω . On the other hand, 3P_0 $q\bar{q}$ -pair creation is modelled by a transition potential V_t , which has two parameters, that is, the universal overall transition intensity λ , and a distance parameter a that is related to the shape of the transition potential. The so-called colour splitting of pseudo-scalar and vector mesons is absorbed in the transition potential through the parameter g_c , at least in the present version of the model.

The four model parameters and the four constituent quark masses for non-strange (either u or d), strange, charm, and bottom quarks are adjusted to the data, i.e., to partial-wave cross sections of meson-meson scattering, or to mesonic bound-state and resonance spectra. Model predictions can then be obtained by giving as input data the relevant quantum numbers, namely flavour, isospin, total angular momentum, parity, and possibly charge conjugation. The outputs of the model are not only predictions for scattering quantities, but also comprise bound-state spectra and corresponding wave functions for the mesonic systems under study.

The philosophy of the model is simple: in the scattering region for a meson-meson scattering process we assume the coexistence of a variety of different systems or channels, that is, one or more confined $q\bar{q}$ pairs, and all combinations of meson-meson pairs that have the correct quantum numbers. For instance, when studying scattering in an isosinglet, we assume that there are definitely non-zero probabilities to find in the interaction region an $n\bar{n}$ pair, an $s\bar{s}$ pair, but also a $\pi\pi$ pair, a $K\bar{K}$ pair, and so forth. The first type of channels differs from the second type in that $q\bar{q}$ pairs are permanently confined, whereas meson-meson pairs feel more modest forces, which might even be neglected in lowest order.

When we describe quarkonia by wave functions ψ_c and two-meson systems by wave functions ψ_f , then we obtain for their time evolution the wave equations

$$(E - H_c) \psi_c(\vec{r}) = V_t \psi_f(\vec{r}) \quad \text{and} \quad (E - H_f) \psi_f(\vec{r}) = [V_t]^T \psi_c(\vec{r}) \quad . \quad (1)$$

Here, H_c describes the dynamics of confinement in the interaction region, H_f the dynamics of the scattered particles, and V_t the communication between the two different sectors.

For the dynamics of confinement we understand here that, as a function of the interquark distance r , the resulting quark-antiquark binding forces grow rapidly outside the interaction region. Consequently, we must eliminate ψ_c from the equations (1), since it is vanishing at large distances and thus *unobservable*. Formally, it is easy to do so. We thus obtain the relation

$$(E - H_f) \psi_f(\vec{r}) = [V_t]^T (E - H_c)^{-1} V_t \psi_f(\vec{r}) \quad . \quad (2)$$

The set of coupled equations (2) for the two-meson channels represented by ψ_f can be solved for the scattering amplitude, either numerically or analytically, once H_c , H_f , and V_t are specified.

2 Fixing the parameters

The two parameters λ and a of the transition potential V_t can be fixed, together with the charm and bottom masses, by the spectra of the $c\bar{c}$ and $b\bar{b}$ vector states. A comparison of model results with experiment is shown in Table (1). In the first column of the table we find the spectroscopic notation for the various states: the first symbol indicates the quarkonium radial excitation $N = \nu + 1$, which for the here employed harmonic-oscillator confinement is related to the total bare quarkonium mass $E_{\ell\nu}$ by

$$E_{\ell\nu} = \omega \left(2\nu + \ell + \frac{3}{2} \right) + \text{quark masses} \quad . \quad (3)$$

In the last column of Table (1) we find the meson-meson channels which are involved in the

$N^{(2s+1)}\ell_J$	$c\bar{c}$		$b\bar{b}$		meson-meson channels involved	
	model	exp.	model	exp.		(L, S)
1^3S_1	3.10	3.10	9.41	9.46	$c\bar{c}$ sector	
2^3S_1	3.67	3.69	10.00	10.02	$DD, D_sD_s,$	(1,0)
1^3D_1	3.80	3.77	10.14	...	$DD^*, D_sD_s^*,$	(1,1)
3^3S_1	4.05	4.04	10.40	10.36	$D^*D^*, D_s^*D_s^*$	(1,0), (1,2) and (3,2)
2^3D_1	4.14	4.16	10.48	...	$b\bar{b}$ sector	
4^3S_1	4.41	4.42	10.77	10.58	$BB, B_sB_s,$	(1,0)
3^3D_1	10.86	10.87	$BB^*, B_sB_s^*,$	(1,1)
5^3S_1	11.15	11.02	$B^*B^*, B_s^*B_s^*$	(1,0), (1,2) and (3,2)

Table 1: Comparison of the model results [8, 9] for $J^{PC} = 1^{--}$ charmonium and bottomonium bound-state masses and resonance central mass positions to experiment [15].

determination of the quarkonia spectra. Vector-vector channels come in pairs, one for total spin zero and one for total spin equal to two. Moreover, spin 2 may combine with F waves. The complete wave function of charmonium (bottomonium) is thus composed of twelve channels, the two $c\bar{c}$ ($b\bar{b}$) channels, one for S wave and one for D wave, coupled to ten meson-meson channels through 3P_0 transitions. Note that not all of these channels are open for the systems under consideration, but that does not necessarily mean their influence is negligible. The relative coupling intensities for the various channels, which follow from the three-meson vertices defined in Refs. [10, 11], are tabulated in Ref. [12]. In Nature, many more meson-meson channels couple in principle, but in the present version of the model only pseudoscalar and vector mesons are considered in the initial and final scattering states, since these are generally the ones that lie close enough to have an appreciable effect.

The non-strange and strange constituent quark masses are fixed by the elastic P -wave $\pi\pi$ and $K\pi$ scattering phase shifts, respectively, as shown in Fig. (2). We observe from the first plot that the agreement between model and experiment is not perfect for larger values of the $\pi\pi$ invariant mass. We believe this to be a consequence of neglecting residual strong forces in meson-meson scattering that are not due to the 3P_0 mechanism, like meson exchange. This might also explain why for $K\pi$ scattering the model gives superior results. Nevertheless, it is remarkable that a

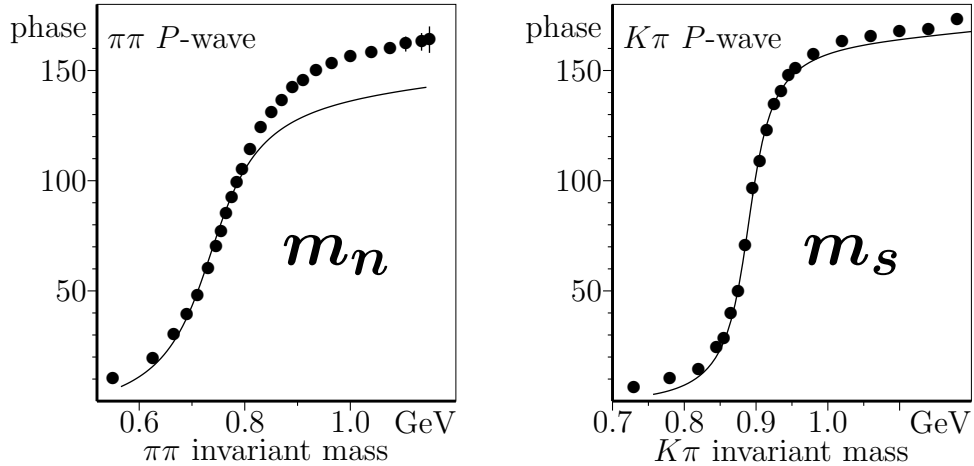


Figure 2: Comparison of the model results (solid lines [8]) for the $\pi\pi$ and $K\pi$ elastic scattering phase shifts with $J^P = 1^-$ quantum numbers to experiment (\bullet), in the energy regions of the $\rho(770)$ and $K^*(892)$ mesons, respectively. The data for $\pi\pi$ are taken from Ref. [13], and for $K\pi$ from Ref. [14].

model which describes the $c\bar{c}$ and $b\bar{b}$ quarkonia bound states and resonances very well, can predict to a fair precision the $\pi\pi$ and $K\pi$ scattering data, just by fixing reasonable values for m_n and m_s . Furthermore, we notice that the correct slopes of the phase shifts at 90° , as a function of the invariant masses, imply the model predicts the right widths for the $\rho(770)$ and the $K^*(892)$.

Finally, the parameter g_c , which accounts for the hyperfine mass splitting of pseudoscalar and vector mesons, is fixed by the mass differences between the $\pi\eta\eta'K$ and $\rho\omega\phi K^*$ nonets. In Table (2) we summarise the model results [8] for the light vector-meson sector. We find good agreement between model and experiment. However, with respect to the radial excitations of the $\rho(770)$ meson, we believe that the particles referred to in Ref. [15], are the D states. In the harmonic-oscillator spectrum a D state is degenerate with the S state belonging to the next radial excitation. Through the coupling to the meson-meson channels the degeneracy is lifted, which gives rise to separate resonances (see Fig. 3 below). Also the $\phi(1680)$ corresponds in our model to the $\phi(1D)$ state.

For the pseudoscalars and the open-charm states, not shown here, the model predictions [8] manifest much more disagreement with the data. Possible causes are a deficient treatment of chiral symmetry, relativity, and pseudothresholds. Further study on these points is clearly required, which is already in course.

state	model	exp.	Ref.	meson-meson channels involved	
	GeV	GeV			(L, S)
$\rho(1S)$	0.76	0.77	[15]		
$\rho(2S)$	1.29	1.29	[17]	$\pi\pi, KK,$	$(1,0)$
$\rho(1D)$	1.40	1.42	[16]	$\pi\omega, \eta\rho, KK^*,$	$(1,1)$
$\rho(3S)$	1.59	1.60	[18]	$\rho\rho, K^*K^*$	$(1,0), (1,2)$ and $(3,2)$
$\rho(2D)$	1.68	1.68	[16]		
$K^*(1S)$	0.93	0.89	[15]	$\pi K, \eta K, \eta' K,$	$(1,0)$
$K^*(2S)$	1.41	1.41	[15]	$\pi K^*, \eta K^*, \eta' K^*, K\rho, K\omega, K\phi,$	$(1,1)$
$K^*(3S)$	1.73	1.72	[15]	$\rho K^*, \omega K^*, \phi K^*$	$(1,0), (1,2)$ and $(3,2)$
$\phi(1S)$	1.03	1.02	[15]	$KK,$	$(1,0)$
$\phi(2S)$	1.53	-		$\eta'\phi, KK^*,$	$(1,1)$
$\phi(3S)$	1.87	-		K^*K^*	$(1,0), (1,2)$ and $(3,2)$

Table 2: Real parts of the singularities in the meson-meson scattering matrices for some of the well-known light vector resonances.

3 Resonances

The overall transition parameter λ provides the communication between permanently closed $q\bar{q}$ channels and meson-meson scattering channels. To lowest order, this describes the decay of a meson, but to higher order also the occurrence of resonances in meson-meson scattering. For $\lambda = 0$, the set of equations (1) describes free, non-interacting two-meson systems with a continuum spectrum above threshold, and confined $q\bar{q}$ systems with a discrete mass spectrum, the so-called *bare* mesons, as given by formula (3) for non-negative integer values of the radial quantum number ν . When λ is non-zero, then, for energies above threshold, the model describes the scattering of interacting two-meson systems, elastic as well as non-elastic, whereas, for energies below threshold, the model describes physical mesons that are stable with respect to OZI decays. A resonance does not represent just one single state, but rather a continuum of states. Each state under the resonance has a different mass, whereby the intensities of its couplings to the different two-meson systems are proportional to the corresponding partial-wave scattering cross sections at that energy. Hence, a resonance should be represented by a whole range of masses, though with varying importance for the scattering data. Such a phenomenon can also be described by a single complex number, namely a singularity in the analytically continued scattering amplitude. For narrow resonances, which here correspond to small values of λ , the real and imaginary parts roughly equal the central resonance mass and half its width, respectively. However, for broad and highly deformed resonances, corresponding to the realm of strong interactions in our model, such simple relations do not exist. It would be helpful if in experiment complex masses could be measured, but exciting the imaginary parts of masses at particle accelerators goes far beyond our imagination as yet. At best, experiment supplies us with partial-wave cross sections, for which scattering amplitudes have to be constructed. Breit-Wigner shapes [19] are the usual techniques, though for strong interactions probably not the most adequate tools. Moreover, since each scattering amplitude has a different pole structure, no generally applicable method exists how to locate singularities. Accordingly, since these poles, with the respective residues, constitute the most relevant information on scattering properties, it would be helpful if the Particle Data Group Collaboration could show us the world averages of full shapes of elastic and inelastic partial-wave cross sections or phase shifts, rather than just the central masses and widths of resonances.

For the time being, it seems that we must content ourselves with at least agreement on the number of scattering-amplitude singularities within large intervals of the invariant mass. For small values of λ , complex poles in the relevant Riemann sheet are expected to lie close to the bare meson masses, whereas for increasing λ the singularities move farther away. Hence, one might expect that their number agrees with the number of bare mesons. Consequently, bound states and resonances could then both be labelled by the spectroscopic quantum numbers, as for instance shown in Table (1). Nevertheless, in the case of the scalar mesons we will see below that not all singularities stem from the bare spectrum.

Bare masses represent bare mesons that result from permanent confinement only. Therefore, models restricted to this particular sector of strong interactions should not adjust their parameters to the bound states and resonances from experiment, although this is common practice unfortunately. In Fig. (3) we depict how the real parts of the poles for the vector charmonium states behave in our model, when λ is varied. For $\lambda = 0$, the bare spectrum of formula (3) is shown. For $\lambda = 1$, one obtains the model result of Table (1). Note that the effect of open-charm channels on the ground state is highly non-perturbative, despite of these channels being all virtual.

Bound states can be represented by special singularities of the scattering amplitude, i.e., poles

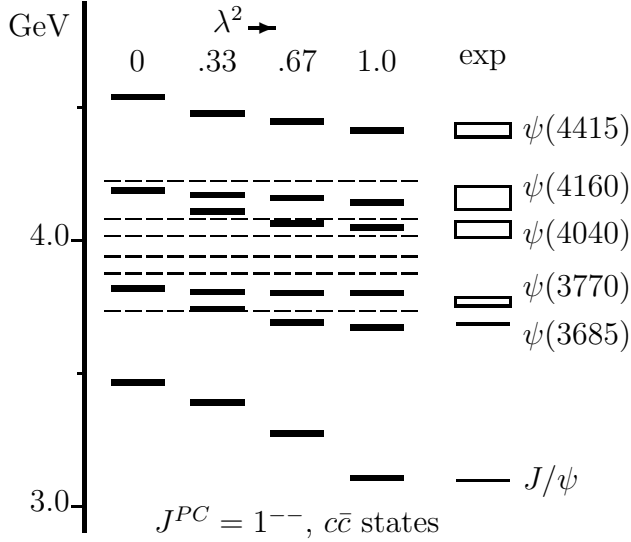


Figure 3: The model results [8, 9] for the central resonance positions of charmonium 3S_1 and 3D_1 states, for four values of the parameter λ , compared to the experimental situation [15]. The various dashed lines indicate the threshold positions of the strong decay channels DD , DD^* , D_sD_s , D^*D^* , $D_sD_s^*$, and $D_s^*D_s^*$.

on the real energy axis below the lowest threshold of the system. The J/ψ (1S) is an example of such a state (see Fig. 3). It consists of two $c\bar{c}$ channels, a dominant one in S wave, the other one in D wave, as well as of channels with virtual pairs of D , D_s , D^* , and D_s^* mesons in P or F waves. The $\psi(2S)$ is an example of a bound state which originates in a bare meson located in the open-charm continuum. For values of λ up to 0.6, the $\psi(2S)$ singularity of the scattering amplitude has an imaginary part, which corresponds to a resonance. But at the $DD\bar{D}$ threshold, the $\psi(2S)$ pole turns real, for $\lambda \approx 0.6$. For the model value of $\lambda = 1$, the singularity is found on the real axis below the $DD\bar{D}$ threshold, in accordance with the physical $\psi(2S)$ state.

4 Scalar mesons

In the foregoing, we have discussed how the parameter λ , which describes the overall intensity of the coupling of $q\bar{q}$ systems to meson-meson scattering channels through the 3P_0 mechanism, can be adjusted to the data. When we carefully inspect wave equation (2), then we observe that the centrifugal barrier is the main contribution of the left-hand side of the equation, whereas the right-hand side is proportional to λ^2 . Consequently, for S -wave scattering, in the absence of a centrifugal barrier, the right-hand side of Eq. (2) dominates the interaction. Now, for low energies far away from the bare states, this term has the form of a potential barrier, in which loosely bound two-meson systems may exist, solely depending on the value of λ . This is exactly what happens for the light flavours. The 3P_0 barrier, not high enough to form bound states, gives rise to a complete nonet of light scalar resonances with central mass positions at about 0.8–1.0 GeV.

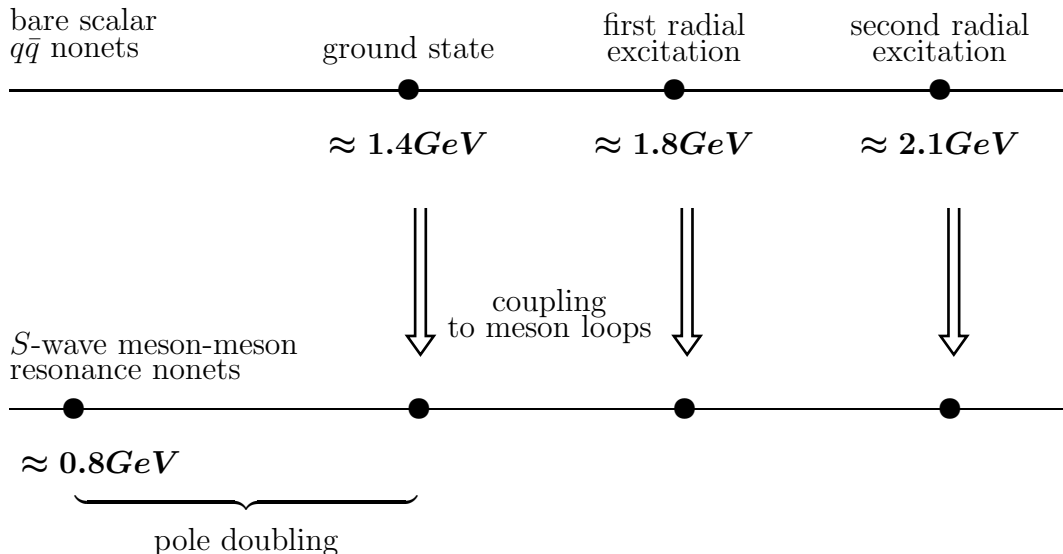


Figure 4: Schematic presentation of pole doubling for the light flavours [6]. Bare meson nonets turn into nonets of mesonic resonances. In the process of switching on the model parameter λ , one extra nonet of singularities appears in the nonet of S -wave meson-meson scattering amplitudes.

For S -wave meson-meson scattering, our model produces, besides an infinity of $J^P = 0^+$ S -matrix poles or resonances, each stemming from a level in the bare spectrum, also one additional singularity that is of a completely different nature. In Fig. (4), we schematically depict this situation. The nonets of scalar resonances are formed by P -wave $q\bar{q}$ states coupled to pseudoscalar-pseudoscalar and vector-vector two-meson channels. There are two isodoublets (non-strange+strange), which among their decay modes have a $K\pi$ channel. Then there is one isotriplet (non-strange+non-strange) involving an $\eta\pi$ channel. And finally there is a system of two isosinglet channels, one for $n\bar{n}$ and one for $s\bar{s}$, which mostly couple to each other through their common $\pi\pi$ and $K\bar{K}$ channels.

Each of the isodoublet states has an extra pole [6] at $727 - i263$ MeV, which corresponds to the two doublets of $K_0^*(830)$ resonances. The three isotriplet states have extra poles [6] at $962 - i28$ MeV, which describe the triplet of $a_0(980)$ resonances. Finally, the coupled system of isosinglets has extra poles [6] at $470 - i208$ MeV and $994 - i20$ MeV, which yield the $f_0(400-1200)$ and $f_0(980)$ resonances, respectively.

The wave functions of the $K_0^*(830)$, $a_0(980)$, $f_0(400-1200)$, and $f_0(980)$ resonances do not have nodes. Consequently, in this sense they must be considered *ground states*. The $a_0(980)$ and $f_0(980)$ resonances are experimentally well established. The $f_0(400-1200)$ resonance is still disputed, whereas the $K_0^*(830)$ has recently been reported in preliminary experimental work [20].

The nonet of resonances stemming from the nonet of ground states of the bare meson spectrum around 1.4 GeV consists of the experimentally established scalars $K_0^*(1430)$, $a_0(1450)$, $f_0(1370)$, and $f_0(1500)$. The higher nonets are still incomplete.

Scalar mesons, especially the light ones, have been the subject of lively debate for several decades. We believe that the here described model has all the necessary ingredients for a reasonable description of the data (see also Ref. [21]).

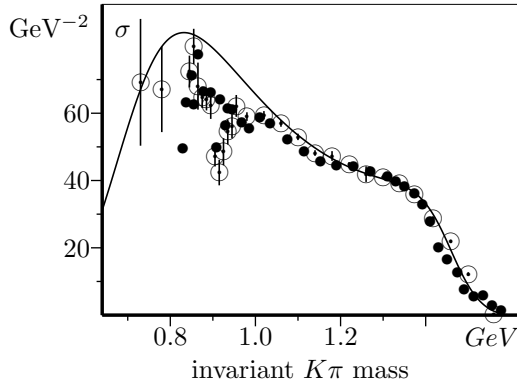


Figure 5: Elastic S -wave $K\pi$ cross section. Data are taken from Refs. [14, 22] (\odot) and [23] (\bullet). The solid line is a model result [4]. Maximum of the theoretical cross section is at 832 MeV.

In Fig. (5), the prediction of Ref. [4] for the S -wave cross section in isodoublet πK scattering is shown. One observes that the central peak lies at 832 MeV. Nevertheless, the related singularity of the πK scattering amplitude we found at $714 - i228$ MeV. Hence, straightforward relations between bumps in the cross section and pole positions do not always exist.

Recently it has been recognised that S -matrix pole positions have more consistency than resonant structures in the data. Values found in the literature for the σ and κ resonances are collected and depicted in Table (3). The world averages for the $f_0(400-1200)$ and $K_0^*(830)$ pole positions, thereby ignoring the differences in the nature of the various analyses, are

$$f_0 [(506 \pm 119) - i(246 \pm 85) \text{ MeV}] ; \quad K_0^* [(786 \pm 78) - i(255 \pm 96) \text{ MeV}] \quad .$$

date	Ref.	σ (MeV)	κ (MeV)
1970	[24]	425 - i 110	
1971	[25]	428 - i 265	
1972	[26]	480 - i 475	
1973	[27]	460 - i 338	665 - i 420
1982	[28]	750 - i 140	800 - i 40
1986	[6]	470 - i 208	727 - i 263
1987	[29]	910 - i 350	
1994	[30]	420 - i 370	
1994	[31]	370 - i 365	
1994	[32]	506 - i 247	
1995	[33]	387 - i 305	
1996	[34]	470 - i 250	absent
1996	[35]	559 - i 185	
1997	[36]	469 - i 179	
1997	[37]	602 - i 196	875 - i 335
1998	[38]	442 - i 227	770 - i 250
1998	[39]	422 - i 213	
1999	[40]	445 - i 235	
1999	[41]	420 - i 317	
1999	[42]	518 - i 261	
1999	[43]	445 - i 221	779 - i 330
1999	[44]		911 - i 158
2000	[45]	498 - i 321	
2000	[46]	732 - i 123	
2000	[20]	478 - i 162	797 - i 205
2000	[47]		708 - i 305
2001	[48]	449 - i 241	
2001	[49]	585 - i 193	905 - i 273
2001	[50]	535 - i 155	
2001	[4]		714 - i 228

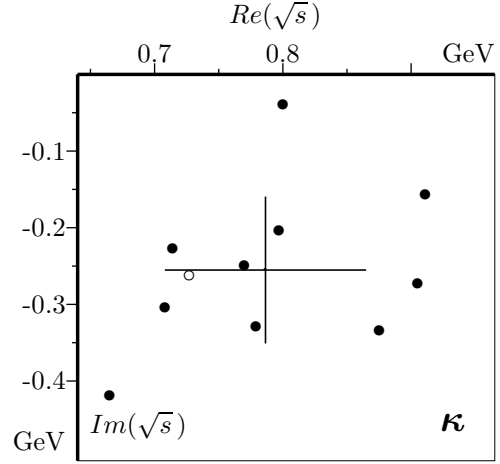
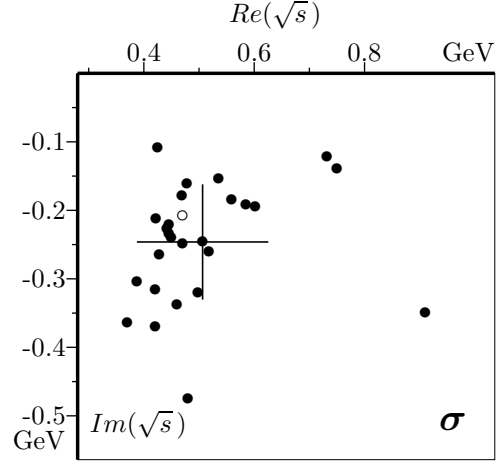


Table 3: Results and references for σ and κ poles in the complex \sqrt{s} plane for isosinglet $\pi\pi$ and isodoublet πK S -wave scattering, respectively. The upper figure shows the locations of the σ poles, the lower one for the κ poles. World averages are indicated in the figures. Our model predictions [6] are indicated by \circ .

5 Radiative transitions

Multichannel wave functions are neither very suitable for figures, nor for comprehensive tables. Radiative decays, however, represent a rather sensitive test for their correctness. Such tests has been carried out in Ref. [51] for the $c\bar{c}$ and $b\bar{b}$ sectors of the model. It involves the development of a formalism for radiative transitions of multicomponent systems with quarkonium and meson-meson channels. In Tables (4) and (5), we compare the theoretical predictions of Ref. [51] for the $c\bar{c}$ and $b\bar{b}$ systems, respectively, with the presently available data.

state	decay product	model [51]	experiment [15]
		keV	keV
$J/\psi(1S)$	$\gamma\eta_c(1S)$	1.67	1.13 ± 0.41
$\psi(2S)$	$\gamma\chi_{c0}(1P)$	31.7	25.8 ± 5.4
	$\gamma\chi_{c1}(1P)$	49.8	24.1 ± 4.9
	$\gamma\chi_{c2}(1P)$	38.5	21.6 ± 4.6
	$\gamma\eta_c(1S)$	1.41	0.78 ± 0.25
$\chi_{c0}(1P)$	$\gamma J/\psi(1S)$	52	98 ± 43
$\chi_{c1}(1P)$	$\gamma J/\psi(1S)$	210	240 ± 52
$\chi_{c2}(1P)$	$\gamma J/\psi(1S)$	228	270 ± 46

Table 4: Comparison of the model results for $c\bar{c}$ radiative transitions to experiment.

state	decay product	model [51]	experiment [15]
		keV	keV
$\Upsilon(2S)$	$\gamma\chi_{b0}(1P)$	1.6	1.7 ± 0.5
	$\gamma\chi_{b1}(1P)$	2.1	3.0 ± 0.8
	$\gamma\chi_{b2}(1P)$	2.6	3.1 ± 0.8
$\Upsilon(3S)$	$\gamma\chi_{b0}(2P)$	1.6	1.4 ± 0.3
	$\gamma\chi_{b1}(2P)$	2.6	3.0 ± 0.6
	$\gamma\chi_{b2}(2P)$	3.1	3.0 ± 0.6

Table 5: Comparison of the model results for $b\bar{b}$ radiative transitions to experiment.

The agreement of the model's predictions with the data is fairly good and has much improved since their publication in 1991, which is an additional argument in favour of the usefulness of the employed formalism.

6 Data analysis

The here described model produces non-exotic bare mesons with all possible angular quantum numbers and an infinity of radial excitations, which, through the universal parameters λ and a , turn into the experimental spectra of all existing mesonic bound states and resonances. However, in spite of the model's success to reproduce a host of experimental data with a very limited number of parameters, it is clearly not suited as a tool for data analysis, owing to the specific model choice of the confining $q\bar{q}$ potential, and furthermore the rather complicated matrix expressions needed to obtain S -matrix-related observables.

In recent work [4], we have indicated how the model's formalism may be applied to data analysis. The bare meson masses and their couplings to the meson-meson channels enter as free fit parameters in this approach. In particular, we have shown that the S -matrix singularities describing the light scalar mesons also appear here. Hence, this simplified model, which can be solved analytically, serves well as a laboratory for studying the general properties of meson-meson scattering. Moreover, for a more detailed description of specific processes, parts of the analytic solutions can be substituted by adjustable parameters.

7 Hybrids

In a recent work [52], Frank Close suggests the use of a model similar to ours for the study of hybrids. Certainly, as the objects which we here call constituent quarks can exchange quark and colour degrees of freedom, one may naturally think of different quark and/or colour configurations. In this sense, also exotic mesonic resonances could, in principle, be accommodated.

8 Conclusions

Bound states and resonances are most conveniently characterised by singularities of the scattering matrix as a function of the total invariant mass. It has the advantage that even in cases where the resonating behaviour of the scattering cross sections is not very clear from experiment, their existence clarifies the classification of well-established resonances into flavour multiplets [3]. However, a disadvantage is that each different theoretical model locates such poles at different complex values. Hence, no agreement can be expected on their positions. Nevertheless, when several analyses, describing the same phenomenon, obtain poles at more or less the same values, like those given in Table (3), then no doubt can exist about their existence in the true model of Nature.

Knowledge about how the poles depend on the parameters of strong interactions in each model could, moreover, lessen the discrepancies. Since it is indispensable to gain experience on the behaviour of mesonic S -matrix singularities, it is useful to dispose of analytical expressions that incorporate most of our knowledge on strong interactions, and are also capable of describing the data to a moderate degree of accuracy. The outlined simplified model serves well for that purpose.

Acknowledgement: This work has been partly supported by the *Fundação para a Ciência e a Tecnologia* of the *Ministério da Ciência e da Tecnologia* of Portugal, under contract numbers POCTI/35304/FIS/2000, and CERN/P/FIS/40119/2000.

References

- [1] H. Yukawa, Proc. Phys. Math. Soc. Jap. **17** (1935) 48.
- [2] J. Schechter, arXiv:hep-ph/0112205.
- [3] E. van Beveren and G. Rupp, talk given at HADRON 2001, Protvino, Russia, August 2001, arXiv:hep-ph/0110156.
- [4] E. van Beveren and G. Rupp, arXiv:hep-ex/0106077.
- [5] E. van Beveren, Nucl. Phys. Proc. Suppl. **21** (1991) 43.
- [6] E. Van Beveren, T. A. Rijken, K. Metzger, C. Dullemond, G. Rupp, and J. E. Ribeiro, Z. Phys. **C30** (1986) 615.
- [7] E. Van Beveren, C. Dullemond, T. A. Rijken, and G. Rupp, Lect. Notes Phys. **211** (1984) 182.
- [8] E. Van Beveren, G. Rupp, T. A. Rijken, and C. Dullemond, Phys. Rev. **D27** (1983) 1527.
- [9] E. van Beveren, C. Dullemond, and G. Rupp, Phys. Rev. **D21** (1980) 772 [Erratum-ibid. **D22** (1980) 787].
- [10] E. van Beveren, Z. Phys. **C17** (1983) 135.
- [11] E. van Beveren, Z. Phys. **C21** (1984) 291.
- [12] E. van Beveren and G. Rupp, Phys. Lett. **B454** (1999) 165 [arXiv:hep-ph/9902301].

- [13] S. D. Protopopescu *et al.*, Phys. Rev. **D7** (1973) 1279.
- [14] P. Estabrooks, R. K. Carnegie, A. D. Martin, W. M. Dunwoodie, T. A. Lasinski, and D. W. Leith, Nucl. Phys. **B133** (1978) 490.
- [15] D. E. Groom *et al.* [Particle Data Group], Eur. Phys. J. **C15** (2000) 1.
- [16] S. Dubnicka, I. Furdik, and V. A. Meshcheryakov, JINR-E2-88-521 (1988).
- [17] D. Aston *et al.*, SLAC-PUB-5606 (1991);
D. Aston *et al.*, Nucl. Phys. Proc. Suppl. **21** (1991) 105.
- [18] L. Chen and W. M. Dunwoodie [MARK-III Collaboration], SLAC-PUB-5674, Presented at Hadron '91 Conf., College Park, MD, Aug 12–16, 1991.
- [19] G. Breit and E. Wigner, Phys. Rev. **49** (1936) 519.
- [20] Carla Göbel, on behalf of the E791 Collaboration, Proceedings of Heavy Quarks at Fixed Target (HQ2K), Rio de Janeiro, October 2000, p. 373–384, arXiv:hep-ex/0012009;
Ibid., Talk given at HADRON 2001, Protvino, Russia, August 2001, arXiv:hep-ex/0110052.
- [21] Kim Maltman, Nucl. Phys. **A675** (2000) 209c;
Ibid., Phys. Lett. **B462** (1999) 14 [arXiv:hep-ph/9906267].
- [22] P. Estabrooks, Phys. Rev. D **19** (1979) 2678.
- [23] D. Aston *et al.*, Nucl. Phys. **B296** (1988) 493.
- [24] J. L. Basdevant and B. W. Lee, Phys. Rev. D **2** (1970) 1680.
- [25] J. L. Basdevant and J. Zinn-Justin, Phys. Rev. **D3** (1971) 1865.
- [26] J. L. Basdevant, C. D. Froggatt, and J. L. Petersen, Phys. Lett. **B41** (1972) 178.
- [27] D. Iagolnitzer, J. Zinn-Justin, and J. B. Zuber, Nucl. Phys. **B60** (1973) 233.
- [28] M. D. Scadron, Phys. Rev. **D26** (1982) 239.
- [29] K. L. Au, D. Morgan, and M. R. Pennington, Phys. Rev. **D35** (1987) 1633.
- [30] N. N. Achasov and G. N. Shestakov, Phys. Rev. **D49** (1994) 5779.
- [31] B. S. Zou and D. V. Bugg, Phys. Rev. **D50** (1994) 591.
- [32] R. Kamiński, L. Leśniak, and J. P. Maillet, Phys. Rev. **D50** (1994) 3145 [arXiv:hep-ph/9403264].
- [33] G. Janssen, B. C. Pearce, K. Holinde, and J. Speth, Phys. Rev. **D52** (1995) 2690 [arXiv:nucl-th/9411021].
- [34] N. A. Törnqvist and M. Roos, Phys. Rev. Lett. **76** (1996) 1575 [arXiv:hep-ph/9511210].

- [35] M. Harada, F. Sannino, and J. Schechter, Phys. Rev. **D54** (1996) 1991 [arXiv:hep-ph/9511335].
- [36] J. A. Oller and E. Oset, Nucl. Phys. **A620** (1997) 438 [Erratum-ibid. **A652** (1997) 407] [arXiv:hep-ph/9702314].
- [37] T. Ishida, M. Ishida, S. Ishida, K. Takamatsu, and T. Tsuru, arXiv:hep-ph/9712230;
S. Ishida, M. Ishida, T. Ishida, K. Takamatsu, and T. Tsuru, Prog. Theor. Phys. **98** (1997) 621 [arXiv:hep-ph/9705437];
S. Ishida, M. Ishida, H. Takahashi, T. Ishida, K. Takamatsu, and T. Tsuru, Prog. Theor. Phys. **95** (1996) 745 [arXiv:hep-ph/9610325].
- [38] J. A. Oller, E. Oset, and J. R. Peláez, Phys. Rev. **D59** (1999) 074001 [Erratum-ibid. **D60** (1999) 099906] [arXiv:hep-ph/9804209].
- [39] M. P. Locher, V. E. Markushin, and H. Q. Zheng, Eur. Phys. J. **C4** (1998) 317 [arXiv:hep-ph/9705230].
- [40] T. Hannah, Phys. Rev. **D60** (1999) 017502 [arXiv:hep-ph/9905236].
- [41] V. V. Anisovich and V. A. Nikonov, arXiv:hep-ph/9911512.
- [42] R. Kamiński, L. Leśniak, and B. Loiseau, Eur. Phys. J. **C9** (1999) 141 [arXiv:hep-ph/9810386].
- [43] J. A. Oller and E. Oset, Phys. Rev. **D60** (1999) 074023 [arXiv:hep-ph/9809337].
- [44] Deirdre Black, Amir H. Fariborz, Francesco Sannino, and Joseph Schechter, Phys. Rev. **D58** (1998) 054012 [arXiv:hep-ph/9804273].
- [45] Z. Xiao and H. Q. Zheng, Nucl. Phys. **A695** (2001) 273 [arXiv:hep-ph/0011260].
- [46] R. Kamiński, L. Leśniak, and K. Rybicki, Acta Phys. Polon. **B31** (2000) 895 [arXiv:hep-ph/9912354].
- [47] Matthias Jamin, José Antonio Oller, and Antonio Pich, Nucl. Phys. **B587** (2000) 331 [arXiv:hep-ph/0006045].
- [48] Q. Ang, Z. g. Xiao, H. Zheng, and X. C. Song, arXiv:hep-ph/0109012.
- [49] K. Takamatsu [Sigma Collaboration], Prog. Theor. Phys. **102** (2001) E52 [arXiv:hep-ph/0012324].
- [50] T. Komada, M. Ishida, and S. Ishida, arXiv:hep-ph/0110357.
- [51] A. G. Verschuren, C. Dullemond, and E. van Beveren, Phys. Rev. **D44** (1991) 2803.
- [52] Frank E. Close, arXiv:hep-ph/0110081.